Anal. Chem. **2002,** *74,* 3540−3546

Simultaneous Multimode Experiments for Studies of Electrochemical Reaction Mechanisms: Demonstration of Concept

Hong-Shik Shim,[†] In-Hyeong Yeo,[‡] and Su-Moon Park*,[†]

Department of Chemistry and Center for Integrated Molecular Systems, Pohang University of Science and Technology, Pohang 790-784, Korea, and Department of Chemistry, Dongguk University, Seoul 100-715, Korea

An instrumental setup has been configured for a simultaneous real time recording of electrochemical, spectroelectrochemical, and mass data on an electrode from a single measurement for studies of complex electrochemical reaction mechanisms. This was achieved by combining a few pieces of equipment: a potentiostat/galvanostat for electrochemical measurements, the near-normal incidence reflectance spectrometer for spectroelectrochemical measurements, and a quartz crystal analyzer (QCA) for mass changes on the electrode. The latter two were coupled through a bifurcated optical fiber on the reflective QCA electrode. The experimental setup thus assembled was demonstrated to be very powerful in elucidating reaction mechanisms of the reaction sequence for a complex reaction, for example, electrochemical oxidation of aniline, which accompanies spectral, as well as weight, changes upon oxidation. The system was also applied to the study of the lithium intercalation reaction of tungsten trioxide thin films in a nonaqueous solution.

INTRODUCTION

Elucidation of the electrochemical reaction mechanism requires more than just conventional electrochemical experiments, in which currents or potentials are measured after an excitation signal of the potential or current is applied to an electrochemical system of interest. For this reason, a number of in situ experiments that can be performed along with the electrochemical experiments have been introduced. These experiments include impedance spectroscopy, electrochemical quartz crystal microbalance (EQCM), ellipsometry, scanning probe microscopy, and spectroelectrochemical techniques of various energy ranges, such as infrared (IR), ultraviolet−visible (UV-vis), and X-ray regions.[1] When used along with electrochemical experiments, these experiments provide additional or complementary information not available from electrochemical experiments alone.

Although one of these in situ experiments can be run rather straightforwardly during an electrochemical experiment, it is difficult, if not impossible, to run more than one during the electrolysis. When two sets of in situ experiments are run separately in order to obtain more than one type of information on an electrochemical system of interest, there could be many variables that are not the same, even under identical experimental conditions. It is thus always preferable to simultaneously obtain more than one piece of information while an electrochemical experiment is run. This concept of "multimode selectivity simultaneously achievable in a single device" for chemical analysis[2] has been presented by Heineman et al. In fact, this concept would be even more applicable to the elucidation of the electrochemical reaction mechanism, which almost always requires more information than that available from just traditional electrochemical experiments. A similar concept has been independently reported by a couple of groups. Mo et al. used simultaneous optical reflectivity and QCA measurements to study the adsorption of bromide on the gold electrode.[3] Xu et al. also reported simultaneous spectroelectrochemical and QCA experiments for their studies on the growth of poly(1-naphthylamine) film.[4] However, these studies were rudimentary in that optical and frequency data were obtained in potential step modes; no full spectral information was obtained in the former,[3] whereas spectra were recorded one at a time at a given potential in the latter.[4]

In our present work, we assembled an experimental setup that allows a full set of electrochemical, spectroelectrochemical, and EQCM data to be obtained in real time. We take advantage of the fact that the near-normal incidence reflectance spectroelectrochemical (NNIRS) experiment[5] can be straightforwardly coupled with the EQCM measurement, because most of the EQCM electrodes have a reflective surface.[6] The system thus assembled has been evaluated on a well-established electrochemical system undergoing changes in both the color and weight, such as electrochemical oxidation of aniline and then applied to a study

* Fax: +82-54-279-3399. E-mail: smpark@postech.edu.
[†] Pohang University of Science and Technology.
[‡] Dongguk University.

(1) For general discussion on these experiments, see, for example, Bard, A. J.; Faulkner, R. L. *Electrochemical Methods*, 2nd ed.; Wiley: New York, 2001; Chapter 11.

(2) (a) Shi, Y.; Slaterbeck, A. F.; Seliskar, C. J.; Heineman, W. R. *Anal. Chem.* **1997**, *69*, 3679. (b) Shi, Y.; Seliskar, C. J.; Heineman, W. R. *Anal. Chem.* **1997**, *69*, 4819. (c) Gao, L.; Seliskar, C. J.; Heineman, W. R. *Anal. Chem.* **1999**, *71*, 4061. (d) DiVirgilo-Thomas, J. M.; C. J.; Heineman, W. R. Seliskar, *Anal. Chem.* **2000**, *72*, 3461.

(3) Mo, Y.; Hwang, E.; Scherson, D. A. *Anal. Chem.* **1995**, *67*, 2415.

(4) Xu, Y.; Xie, Q.; Hu, M.; Nie, L.; Yao, S. *Electrochim. Acta* **1995**, *389*, 85.

(5) (a) Pyun, C.-H.; Park, S.-M. *Anal. Chem.* **1986**, *58*, 256. (b) Zhang, C.; Park, S.-M. *Anal. Chem.* **1988**, *60*, 1639. (c) Zhang, C.; Park, S.-M. *Bull. Korean Chem. Soc.* **1989**, *10*, 302.

(6) Buttry, D. A. In *Electroanalytical Chemistry*; Bard, A. J., Ed.; Marcel Dekker: New York, 1991; Vol. 17, pp 1−86.

10.1021/ac020121c CCC: $22.00
Published on Web 06/11/2002

of the intercalation of Li^+ into the tungsten oxide thin film. When properly configured, the system would be very powerful in elucidating reaction mechanisms for a sequence of chemical reactions during a single electrochemical experiment.

EXPERIMENTAL

Chemicals used in the experiments were of reagent grade, and the solutions were prepared using doubly distilled, deionized water. Aniline (Aldrich), lithium perchlorate ($LiClO_4$, Aldrich, 99.99%), and tungsten trioxide powder (WO_3, Aldrich 99.995%) were used as received. Propylene carbonate (Aldrich) was used after drying over molecular sieves for a few days, followed by fractional distillation under an inert atmosphere. The tungsten trioxide thin film with a thickness of ~160 nm was prepared by the thermal vapor evaporation method on the platinum coated quartz crystal electrode (Seiko EG&G) for quartz crystal microbalance measurements. The WO_3 film thus obtained was annealed at 350 °C for 2 h.

A three-electrode system housing a platinum-coated working electrode with or without a WO_3 film, a platinum foil counter electrode, and a Ag|AgCl (in saturated KCl) (for an aqueous solution) or a lithium foil (for a nonaqueous solution) reference electrode was used. The platinum-coated quartz crystal working electrode was mounted in a cell specifically designed such that the combined part of a bifurcated optical fiber probe is located perpendicular to the reflective QCA electrode through a hole on the wall facing the electrode for simultaneous spectroelectrochemical and EQCM experiments. Thus, the optical fiber probe tip faces the reflective working electrode perpendicular to it at a distance of ~3−5 mm. All of the experiments were carried out under an argon atmosphere.

The electrochemical and the EQCM measurements were carried out with an EG&G model 273A potentiostat/galvanostat and a Seiko EG&G model 917 quartz crystal analyzer (QCA), respectively. An AT-cut, 9 MHz platinum-plated quartz crystal (Seiko EG&G model QA-A9M-AU, 0.20 cm^2) was used as a resonator and a working electrode. The QCA, the potentiostat/galvanostat, and the computer were connected through a GPIB interface card, which was controlled by EG&G PAR 270/250 electrochemistry software. The frequency change, Δf, has the following relationship[6] with the mass change, Δm.

$$\Delta m = -C\Delta f \qquad (1)$$

The frequency recorded at the outset of each experiment was taken as a base frequency, from which the Δf values were calculated when the system was being perturbed electrochemically.

The spectroelectrochemical setup has been described elsewhere in the literature.[5] The UV−vis absorption spectra were taken with an Oriel InstaSpec IV spectrometer with a charge-coupled device (CCD) array detector, which was configured in a near-normal incidence reflectance mode using a bifurcated quartz optical fiber. The wavelength of the spectrograph was calibrated using a small mercury lamp. The operation of three separate instruments, that is, EG&G model 273A potentiostat/galvanostat, the Seiko EG&G model 917 QCA, and the Oriel InstaSpec IV spectrometer was synchronized so that electrochemical, EQCM, and spectroelectrochemical data were obtained simultaneously.

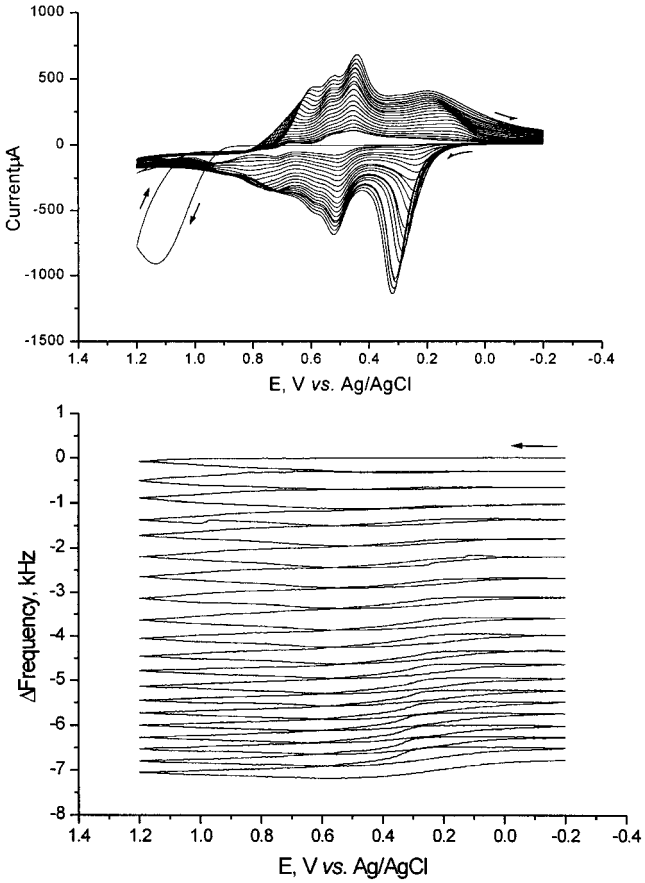

Figure 1. (a) Series of cyclic voltammograms recorded during electrochemical polymerization of aniline by a potentiodynamic method at a scan rate of 50 mV/s in a 0.50 M H_2SO_4 solution containing 0.030 M aniline and (b) the frequency change recorded concurrently during the potentiodynamic growth of polyaniline (PAn).

RESULTS AND DISCUSSION

Because of the relatively fast recording capability of the spectrometer once every 25 ms, a full range of spectra can be recorded while both EQCM and electrochemical data are acquired. To show the capability of the system, a relatively well understood electrochemical reaction system, that is, polymerization of aniline, was used to evaluate the multimode experimental system. When aniline is oxidized in an acidic solution, polyaniline (PAn) is produced, forming a highly colored film on the electrode surface along with causing an increase in weight.[7] Figure 1 shows a series of cyclic voltammograms (CVs) (a) and accompanying frequency decreases (b) for the formation of the PAn in an aqueous solution containing 0.030 M aniline and 0.50 M H_2SO_4 when the potential was scanned repeatedly between −0.20 and 1.20 V vs the Ag|AgCl electrode. Figure 2 presents a number of spectra recorded every 50 mV (i.e., every 1 s) during the first cycle while the potential was scanned. Although we could have obtained the spectra for the whole 20 cycles, we recorded spectra

(7) (a) Stilwell, D. E.; Park, S.-M. *J. Electrochem. Soc.* **1988**, *135*, 2254. (b) Zotti, G.; Cattarin, S.; Comisso, N. *J. Electroanal. Chem.* **1988**, *239*, 387. (c) Park, S.-M. In *Handbook of Conductive Molecules and Polymers*; Nalwa, H. S., Ed.; Wiley: Chichester, England, 1997; Vol. 3, pp 429−469.

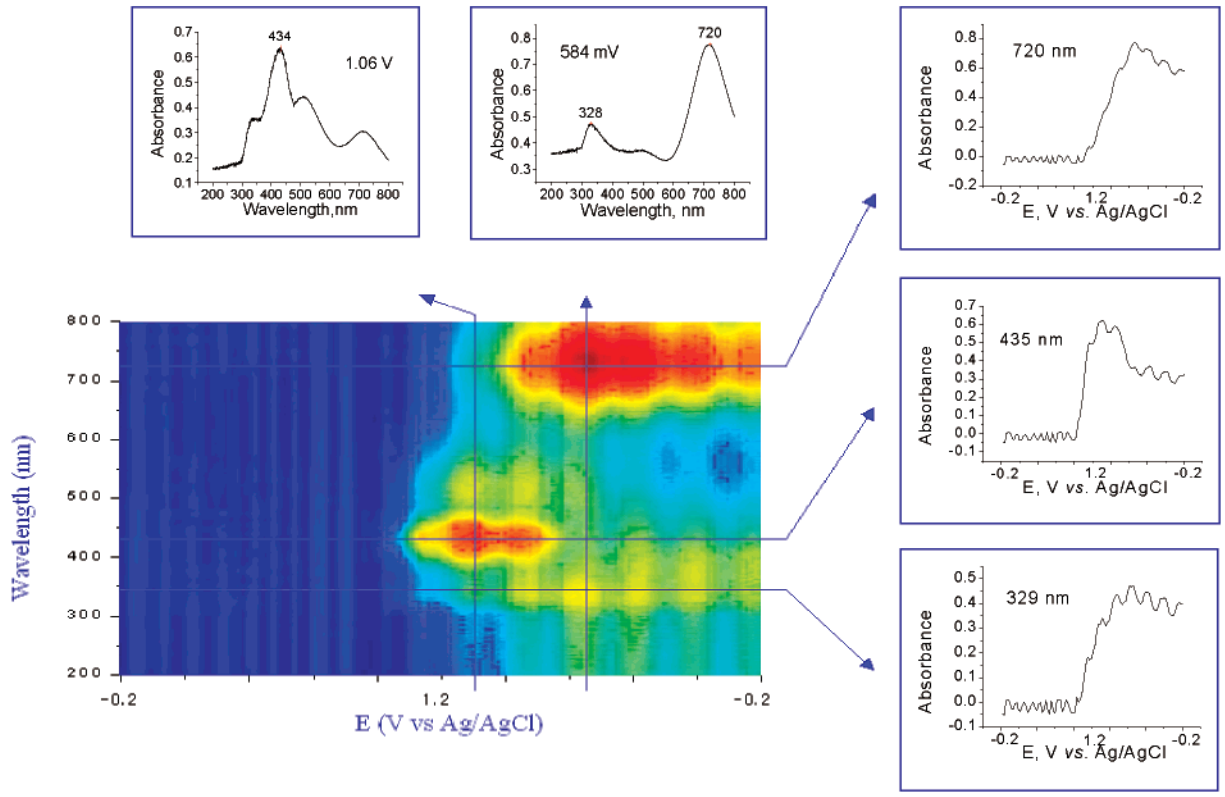

Figure 2. Contour diagram for absorbance vs wavelength as well as vs potential recorded concurrently with those shown in Figure 1 for only the first cycle and (clockwise from top left) the snapshots of the absorption spectrum at 1.06 and 0.584 V and voltabsorptograms at 720, 435, and 329 nm, respectively.

only during the first full cycle. It is seen from the figures that all three forms of data, that is, electrochemical (CVs), weight increases (frequency changes), and spectral changes, are recorded concurrently in real time.

Figure 1a shows that aniline is oxidized, and its CV peak current is observed at ~1.15 V during the first cycle. No more aniline oxidation peak current is observed after the first scan; only the PAn film formed during the first cycle is seen to be oxidized. This is well-understood in terms of the autocatalytic mechanism for the formation of PAn,[7] and we do not elaborate on it here. During the 20 cycles, the frequency continues to decrease, indicating that the weight of the PAn film keeps increasing. By analyzing the pattern of the frequency decrease, one can see how the PAn film grows and how the counterions go in and out during the doping-dedoping processes while the potential is scanned.[8] For example, the $d(\Delta f)/dt$ vs potential (E) plot can be obtained from the curves shown in Figure 1b and compared with the corresponding CV curves. The $d(\Delta f)/dt$ vs E plot should be identical to the CV, provided that aniline oxidation leads quantitatively to the weight increase. These analyses, along with spectroscopic information obtained simultaneously, would allow the polymer growth reaction mechanism to be elucidated.[8c]

Figure 2 shows a pseudocolor plot of a function of two variables in which a large number of full-frame spectra are shown as a function of potential swept, along with a few snapshots at specified potentials (top) or wavelengths (right). The snapshot recorded at 435 nm, which represents a voltabsorptogram for this species,[5b,c] shows that an oxidation product absorbing at this wavelength begins to absorb from ~0.92 V and reaches a maximum at ~1.1 V on the reverse scan. Apparently, the species generated first upon aniline oxidation must be the radical cation of a dimeric form, benzidine, which evolves into the longer polymer with its backbone absorbing at 329 nm and the oxidized form of the polymer absorbing at 720 nm.[9] The two bands, one at 329 nm and the other at 435 nm, behave in an identical manner and reach their maximum intensity (or concentrations) at ~0.68 V during the reverse scan. These observations indicate that the oxidized species of the dimers evolve into the longer polymer chain; the fluctuations in the absorbance values reflect their relative concentrations due to a series of proposed reactions for PAn growth[7a,c]

$$(\mathrm{An})_n^{\mathrm{red}} \rightarrow (\mathrm{An})_n^{\mathrm{ox}} + ne^- \qquad (2)$$

$$(\mathrm{An})_n^{\mathrm{ox}} + \mathrm{An} \rightarrow \rightarrow \rightarrow (\mathrm{An})_{n-1}^{\mathrm{ox}}(\mathrm{An})_2^{\mathrm{red}} \qquad (3)$$

in which the reduced PAn is first oxidized, followed by the chain-lengthening reaction, rendering part of the chain to a reduced state. This autocatalytic reaction requires the oxidized and reduced states fluctuate, which is shown to take place by the voltabsorptograms at 329 and 720 nm. When the number of the chain, n, is

(8) (a) Orata, D.; Buttry, D. A. *J. Am. Chem. Soc.* **1987**, *109*, 3574. (b) Cui, S.-Y.; Park, S.-M. *Synth. Met.* **1999**, *105*, 91. (c) Lee, H. J.; Cui, S.-y.; Park, S.-M. *J. Electrochem. Soc.* **2001**, *148*, D139. (d) Choi, S.-J.; Park, S.-M. *J. Electrochem. Soc.* **2002**, *149* (2), E26.

(9) (a) Shim, Y.-B.; Won, M.-S.; Park, S.-M. *J. Electrochem. Soc.* **1987**, *137*, 538. (b) Won, M.-S.; Shim, Y.-B.; Park, S.-M. *Bull. Korean Chem. Soc.* **1992**, *13*, 680.

small, which would be the case during the first potential cycle, that is, an early stage of the polymer growth, the fluctuations would be significant, as shown in these voltabsorptograms. The fluctuation in absorbance values at 435 nm after a fast rise to a maximum value suggests that the concentration of the oxidized dimer species fluctuates as a result of the subsequent chemical reactions when their concentrations reach a critical value to couple with monomeric species. Although this sequence of polymer growth mechanism has been proposed,[7c] this is the first time that the whole reaction sequence has been actually observed.

From the two snapshots at given potentials, that is, one recorded at 1.06 V and the other at 0.584 V, both during the reverse scan, we can see what is the major species produced at those potentials. At 1.06 V during the forward scan, we see that the dimeric species absorbing at 435 nm has the highest concentration, with part of them already starting to become longer-chain polymers, as indicated by the emergence of the absorption peaks at ~320 and 710 nm. These peaks were assigned to be the neutral form of PAn with its $n-\pi^*$ absorption (~320 nm), the cations of dimeric forms (435 nm), and the oxidized form (polaron) of PAn of the relatively shorter chain polymer (710 nm). Notice again that the wavelengths for maximum absorbances are shorter than those observed in later stages for these species. This is because the chain lengths are relatively short at this early stage. During the reverse scan, it is seen that only absorption corresponding to the $n-\pi^*$ absorption of the neutral PAn of relatively short chain at ~329 nm and the radical cations of PAn (polaron) at ~730 nm are observed with the peak at 435 nm almost completely suppressed.[9,10] These observations indicate that the species absorbing at 435 nm evolves into those absorbing at 329 and 720 nm, as already pointed out above.

It is seen clearly from these results that a full range of electrochemical, spectroelectrochemical, and weight change data can provide new insight into the reaction mechanism. One may also recast the above data in the form of a derivative cyclic voltabsorptometry (DCVA) plot by taking the first derivative of the absorbance values with respect to time, that is, dA/dt, and compare with the corresponding CVs.[5b,c,11] The DCVA curve reflects the rate of formation of a species responsible for absorption upon change in potential, just as the $d(\Delta f)/dt$ plot indicates the rate of weight change upon change in potential.[8c,e] When the current efficiency is 100% for the formation of the species absorbing at a specific wavelength, the DCVA curve should be exactly the same as the CV recorded simultaneously. Comparison of the CV, DCVA, and $d(\Delta f)/dt$ curves, as well as their integrated forms, leads to a number of clues for the elucidation of the mechanisms involved.

The electrochemical quartz crystal microbalance (EQCM) data shown in Figure 3 are just the magnified version of those shown in Figure 1b. From the frequency change data recorded during the first cycle, a very small weight increase begins to be observed from ~0.625 V, which would represent the adsorption of aniline molecules on the electrode surface.[12] The sizable weight increase begins to be observed from ~0.97 V, which is more positive than the potential (0.92 V) where the 435-nm absorption peak starts to show up. The delay in weight increase compared to the increase in absorbance shown here indicates that the coupling of oxidized dimers with aniline monomers starts to occur when their concentration reaches a critical value for formation of the corresponding polymer. The weight continues to increase as a result of the active coupling of the oxidized species generated at above ~0.90 V until the potential goes below to ~0.41 V during the reverse scan, where it levels off down to 0.29 V. The weight then starts to decrease, albeit slightly. The decrease in weight reflects the ejection of counteranions upon reduction of the oxidized polymer. A more quantitative analysis of the frequency change data during the PAn growth has been made.[8d] Here, we only wish to point out that the weight increase shows significant delays as compared to the emergence and decay of the corresponding absorption peaks due to relatively slow polymerization reaction kinetics. This has been confirmed by a number of scan-rate-dependency experiments.

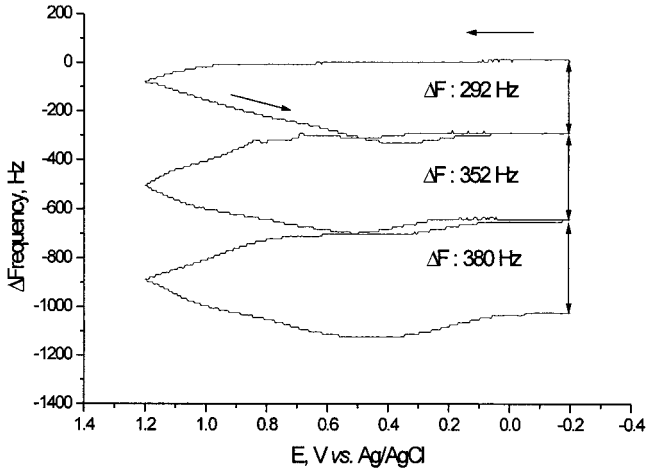

Figure 3. Frequency changes recorded for the first three cycles. The data were taken from Figure 1b.

The second electrochemical reaction we examined was the intercalation of lithium into the tungsten oxide film in nonaqueous solutions. The reaction is expressed as[13]

$$WO_3 + xLi^+ + xe^- \rightarrow Li_xWO_3 \qquad (4)$$

where x would be ~0−1.0. This reaction has been studied extensively as an electrochromic reaction in both aqueous and nonaqueous media for proton and lithium intercalation, respectively.[13] This reaction accompanies changes in both the color and the weight, depending on whether the alkali metal ions or the protons are intercalated.

Figure 4 shows a series of CVs recorded for three cycles. Two steps of intercalation are noticed, as indicated by the CV peaks at ~2.7 (a) and 2.3 V (b), respectively. The presence of two CV peaks suggests that there must be two energetically different sites for lithium intercalation, as is the case for the lithium intercalation into the graphite lattice, which also undergoes a few steps of intercalation reactions.[15] The two different sites might have

(10) Stilwell, D. E.; Park, S.-M. *J. Electrochem. Soc.* **1989**, *136*, 427.
(11) Bankroft, E. E.; Sidwell, J. S.; Blount, H. N. *Anal. Chem.* **1981**, *53*, 1390.
(12) (a) Holze, R. *Electrochim. Acta* **1987**, *32*, 1527. (b) Holze, R. *J. Electroanal. Chem.* **1987**, *224*, 253. (c) Holze, R. *J. Electroanal. Chem.* **1988**, *250*, 143.
(13) Granqvist, C. G. *Handbook of Inorganic Electrochromic Materials*; Elsevier: Amsterdam, 1995.
(14) Granqvist, C. G. *Handbook of Inorganic Electrochromic Materials*; Elsevier: Amsterdam, 1995, Chapters 2−11.

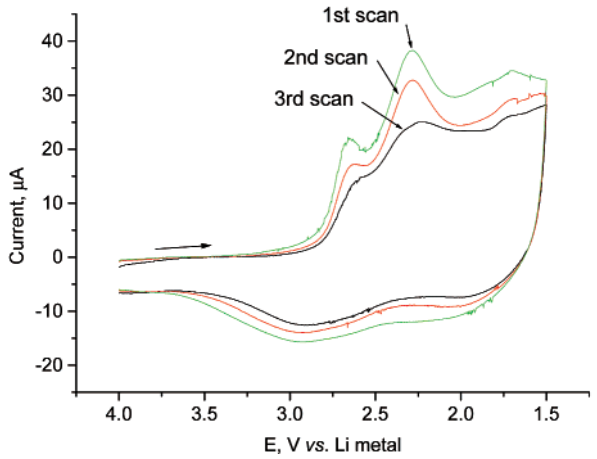

Figure 4. Cyclic voltammograms recorded at a tungsten trioxide thin film on a platinum-covered quartz crystal electrode in a 1.0 M $LiClO_4$ solution. The scan rate was 5 mV/s.

resulted from an incomplete annealing of the film. The presence of two different energy states will be shown again below by the spectra recorded during the electrochemical intercalation reaction. In addition, the decrease in CV peak currents with the scan number suggests that the intercalation/deintercalation process becomes irreversible upon repeated scanning. The lithium ions that have been intercalated into the second level of the energy state are not readily released upon anodic scanning, as will be discussed below. Finally, the lower energy state observed at 2.7 V merges into the higher energy states upon repeated scanning, suggesting that the film is electrochemically annealed upon repeatedly scanning the potential.

To get more quantitative insights into the intercalation/deintercalation reactions, the reactions at two intercalation potentials, that is, 2.7 and 2.3 V, as well as the deintercalation processes at 4.0 V, were studied potentiostatically. From the CVs shown in Figure 4, we chose 2.5 and 2.0 V for cathodic steps for Li^+ intercalation into the two states and 4.0 V for anodic steps for complete deintercaltion from both intercalated states. Figure 5 shows a chronoamperometric curve for intercalation at 2.5 V (a), the corresponding charges and frequency decreases for intercalation (b), and charges and frequency decreases recorded during deintercalation at 4.0 V (c). The charges, which were simply obtained by integrating the currents, should take the same form as the frequency decreases, which reflect the weight increase and should, thus, be the integrated form. Both forms follow almost exactly the same trace during the early stage of the intercalation process, but they deviate slightly in the later stage.

The mass increase determined from the frequency decrease is smaller than that calculated from the charge. The total charge calculated for the forward process for 300 s after the potential step to 2.5 V was 12.8 mC ($= 9.31 \times 10^{-7}$ g Li) for the frequency decrease of 169 Hz ($= 2.26 \times 10^{-7}$ g Li) during the intercalation process, whereas the corresponding total anodic charge was 13.0 mC for the frequency decrease for 162 Hz when the $LiWO_3$ was reoxidized at 4.0 V. Here, we see that the amount of lithium ion

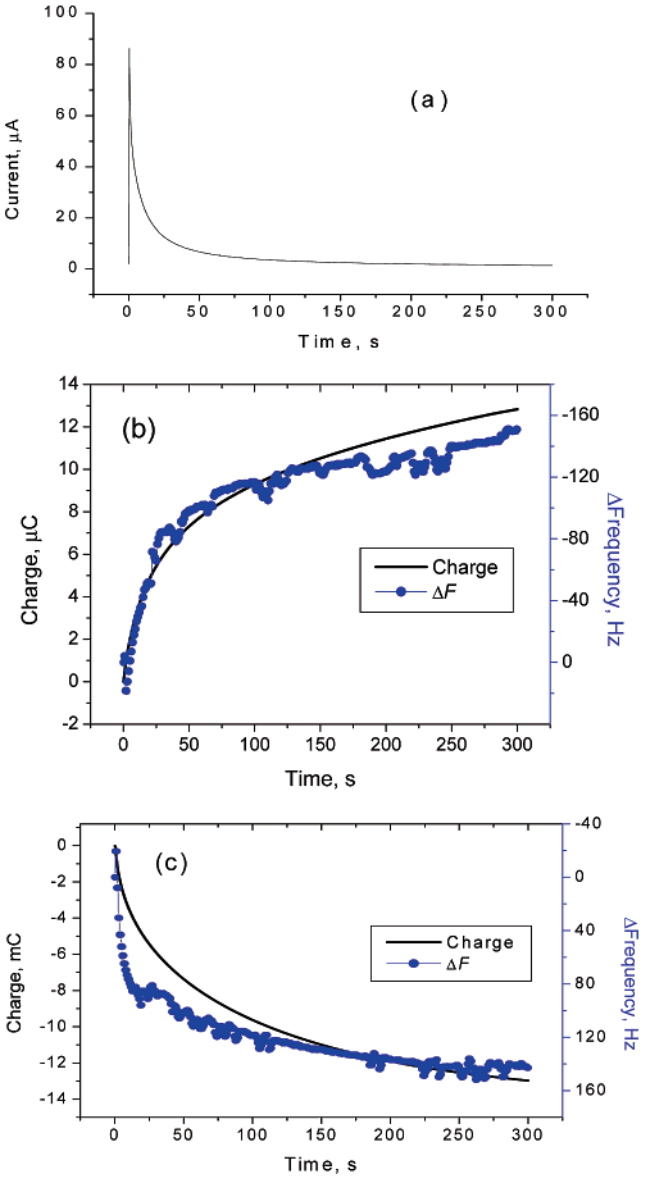

Figure 5. (a) Chronoamperogram recorded for intercalation of lithium ion at a stepped potential of 2.50 V vs Li, (b) corresponding charges (solid line) and frequency changes (●) vs time, and (c) anodic charges (solid line) and frequency changes (●) recorded for deintercalation of preintercalated lithium ions at 4.0 V.

intercalated is much smaller than that calculated from the charge passed, which was attributed to the antagonistic processes, that is, insertion of Li^+ (faradaic process) and expulsion of ClO_4^- (nonfaradaic process), occurring during the cathodic intercalation.[16] The nonfaradaic process is reported to be associated with the expulsion of anions on the electrode surface under the electric field effect.[16] Although the reversibility is good based on recovery of both the charge (101%) and the weight (96.9%), some lithium ions are still in the crystal lattice in an ionic form, even after oxidation. This is probably the reason for the capacity loss during the second and third cycles in the CVs, as shown in Figure 4.

(15) (a) Dahn, J. R. *Phys. Rev.* **1991**, *44*, 9170. (b) Ohzuku, R.; Iwakoshi, Y.; Sawai, K. *J. Electrochem. Soc.* **1993**, *140*, 2490. (c) Piao, T.; Park, S.-M.; Doh, C.-H.; Moon, S.-I. *J. Electrochem. Soc.* **1999**, *146*, 2794. (d) Kim, Y.-O.; Park, S.-M. *J. Electrochem. Soc.* **2001**, *148*, A194.

(16) (a) Bohnke, O.; Vuillemin, B.; Gabrielli, C.; Keddam, M.; Perrot, H.; Takenouti, H.; Torresi, R. *Electrochim. Acta* **1995**, *40*, 2755. (b) Bohnke, O.; Vuillemin, B.; Gabrielli, C.; Keddam, M.; Perrot, H. *Electrochim. Acta* **1995**, *40*, 2765.

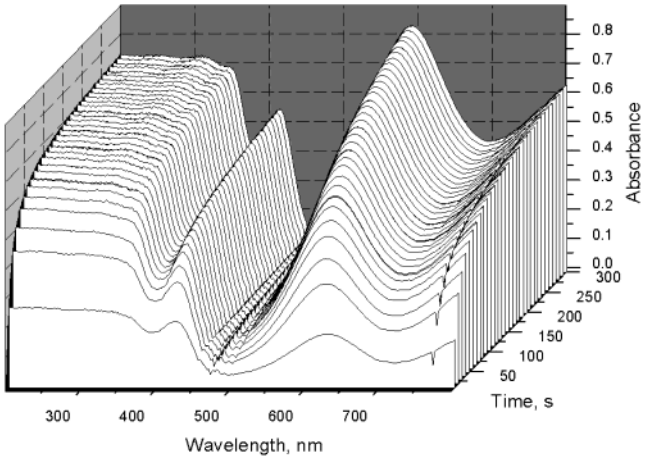

Figure 6. Series of spectra recorded during lithium deintercalation at 4.0 V for 300 s. Spectra were recorded every 10 s.

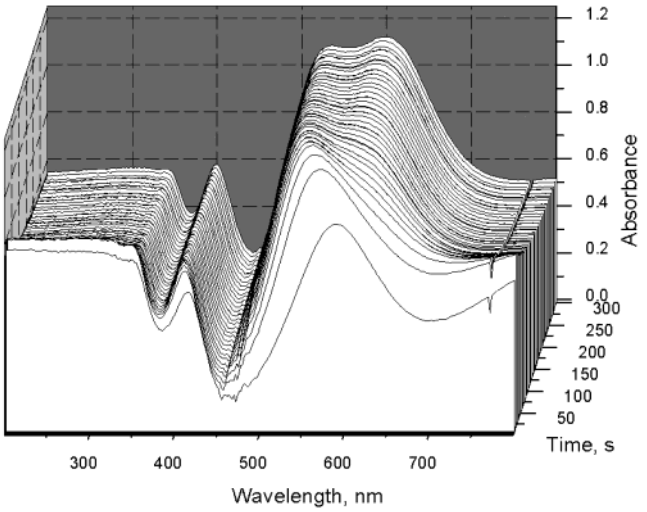

Figure 7. Series of spectra recorded during lithium intercalation at 2.0 V for 300 s. Spectra were recorded every 10 s.

When the potential was stepped to 2.0 V for 300 s, the charge injected into the WO_3 film increased to 34.4 mC, with a frequency decrease of 357 Hz (Figure 5c). The current efficiencies for lithium intercalation are even poorer here at 2.0 V than at 2.5 V. Upon reversing the potential back to 4.0 V, the recovered charge was only 27.7 mC, with a frequency increase of 310 Hz. These correspond to 80.7 and 86.8% with respect to the charge and mass reversibility, respectively, as compared to 100 and 96.9% in the case when the stepped potential was 2.5 V. It is interesting that the mass reversibility is better than the charge reversibility here, in contrast to the case at 2.5 V; this suggests that the current corresponding to the nonfaradaic process is larger during the cathodic step than during the anodic step, particularly in the later stage of deintercalation. Another point to note is that a significant amount of intercalated lithium ions into the higher energy state appears to fit better into the WO_3 crystal lattice. In other words, the reversibility of the process became significantly deteriorated when the stepped potential was more negative.

The presence of two energetically different states is demonstrated by a series of spectra recorded concurrently while both electrochemical and EQCM experiments were run. A series of spectra obtained every 10 sec during the intercalation process are shown in Figure 6. The absorbance increases rapidly at the beginning, and the rate of increase slows as the sites become saturated. Here, we see that the absorption bands at ~300, 405, and 600 nm increase monotonically upon intercalation. These bands should be the band gap transition of the 2p electrons from the valence band of oxygen to various levels of the 5d conduction bands of $LiWO_3$,[17] in which tungsten is in the 5+ state. Upon oxidation (or deintercalation) of the intercalated lithium ions, the spectrum returns to the baseline with almost no residual absorbance (spectra not shown).

Figure 7 shows the spectra recorded while the WO_3 film was being intercalated at 2.0 V for 300 s. We see from the spectra that the spectral bands at longer wavelengths began to split into two peaks at ~550 and 650 nm from starting at ~25 s. This perhaps results from the splitting of the conduction band due to the lithium ions injected into the lattice, depending on how much the 6s electron shell of the tungsten is filled, resulting in two different energy states, as described above. Upon deintercalation, the spectra with the two absorption peaks undergo a reverse change to the spectra with single absorption peaks as the Li^+ concentration goes down, but the film did not recover a completely bleached state of no absorbance (spectra not shown); instead, the maximum absorbance value remained at ~0.25 after 300 s of discharge at 4.0 V. The remaining spectrum after 300 s at 4.0 V was essentially the same as that shown in Figure 6, indicating that there is only one energy state at lower Li^+ concentrations. The high energy state does exist only at higher Li^+ concentrations, which reverses to the low energy state as much of the Li^+ is deintercalated. Thus, some lithium ions fill in interstitial space and are not ejected from the lattice, which causes the irreversibility of the process. When the spectra were recorded in the same way as for Figure 2, results that were very similar to those shown in Figures 6 and 7 were obtained, except that the spectra were more cluttered.

Despite many studies on the optical properties of WO_3 reported during intercalation/deintercalation processes,[13] this is the first report on the two energetically different states of WO_3 depending on how much Li^+ has been intercalated. The results obtained from the multimode experiment on intercalation/deintercalation of Li^+ clearly show what has not been reported thus far.

CONCLUSION

We have constructed a system that allows multimode information to be obtained from a single device by combining the spectroelectrochemical system with the EQCM experiment. This technique would serve as a very powerful tool for studying an electrochemical reaction undergoing changes in both the color and weight. There are numerous electrochemical reaction systems that accompany both color and weight changes upon excitation by an electrochemical signal. In our present work, we have demonstrated by taking two reasonably well understood reaction systems that new insights can be obtained by simultaneously recording three different types of in situ signals. The series of spectra recorded while the potential is being swept provide a pseudocolor plot of the absorbance for two variables for a

(17) Rougier, A.; Portemer, R.; Quédé, A.; El Marssi, M. *Appl. Surf. Sci.* **1999**, *153*, 1.

sequence of reactions along with the weight change data, which provide additional/complimentary information for the elucidation of the reaction mechanism. This would have been impossible without such an experiment.

ACKNOWLEDGMENT

This work was supported by a grant from the Korea Science and Engineering Foundation (KOSEF) through the Center for Integrated Molecular Systems at Pohang University of Science and Technology, and graduate stipends were provided to H.S.S. by the Korea Research Foundation through the BK21 program.

Received for review February 25, 2002. Accepted April 30, 2002.

AC020121C